

## Oldest (3.5 Ga) Zircons of the Urals: U–Pb (SHRIMP-II) and $T_{DM}$ Constraints

Yu. L. Ronkin<sup>a</sup>, S. Sindern<sup>b</sup>, Corresponding Member of the RAS A. V. Maslov<sup>a</sup>,  
D. I. Matukov<sup>c</sup>, U. Kramm<sup>b</sup>, and O. P. Lepikhina<sup>a</sup>

Received March 3, 2007

DOI: 10.1134/S1028334X07060074

The Archean domains of the Earth composed of granite–greenstone and granulite–gneiss associations are now sufficiently well studied. Nevertheless, many aspects related to the early history of the planet are still far from being solved [1, 2, and others]. Such a situation is also characteristic of the Uralian foldbelt. The formation of the crust in this region spanned a long period comprising the Archean–Early Proterozoic, Late Proterozoic, Paleozoic, and post-Paleozoic stages [3]. In recent years, considerable progress has been achieved in reconstruction of the major features of the last three stages in the foldbelt evolution mainly due to the active introduction of advanced methods of isotope geology based on sophisticated analytical equipment into geological studies. At the same time, significant difficulties remain in the reconstruction of the pre-Riphean stage for the following reasons: first, the reliably defined Archean metamorphic domain in the Urals is extremely limited and represented, in fact, only by the Taratash polymetamorphic complex of the Central Uralian Uplift with the single Neoproterozoic date [4] obtained only recently by the classical U–Pb zircon method; second, the dating of Neoproterozoic rocks is hampered by several methodological and analytical problems, the correct solution of which is essential for validity of the results obtained.

The Taratash polymetamorphic complex is located among volcanosedimentary rocks of the Lower Riphean Ai and Satka formations at the junction of the Bashkir and Uraltau anticlinoria located between the South and Middle Urals (Fig. 1). It occupies an area of 400 km<sup>2</sup> and is composed of lithologically variable

gneisses, two-pyroxene crystalline schists, quartz-bearing diorites and gabbrodiorites, and quartz–feldspar rocks. The geological structure of the Taratash Complex, the petrology of its rocks, and metamorphism evolution are described in detail in [5].

The history of the study of the Taratash Complex by methods of isotopic geology (K–Ar,  $\alpha$ -Pb,  $^{207}\text{Pb}/^{206}\text{Pb}$  thermal isochron, and classical U–Pb) is already more than 35 years old [4–7]. These studies revealed several stages in the evolution of the rock complex corresponding to granulite metamorphism, high-temperature amphibolite-facies diaphthoresis, amphibolite-facies metamorphism, and greenschist diaphthoresis. Nevertheless, many aspects of its formation remain unclear. Moreover, they are conflicting to a significant extent in light of recent data [8].

The U–Pb ID-TIMS dates obtained for single zircons from the leucosome of Taratash migmatites and granites [8] show a lack of crystals older than  $2344 \pm 29$  Ma. Using the classical U–Pb method, KrasnobaeV and Cherednichenko [4] obtained an older date ( $2915 \pm 155$  Ma) for zircons from two-pyroxene crystalline schists, augen gneisses, and injection gneisses of the Taratash Complex. However, significant weighted portions of zircon (6.5–11.2 mg) were used in the work cited above. Taking into consideration the negative correlation ( $r = -0.73$ ) between the zircon sample weight and  $^{207}\text{Pb}/^{206}\text{Pb}$  ages; the great diversity of mineralogical features of the analyzed zircon crystals (presence of at least three generations and distinct inherited cores); and lack of special techniques of sample preparation, such as air abrasion and/or acid treatment, which make it possible to differentiate the analyzed material, coordination of the dating mentioned above with the real geological event becomes a debatable issue.

It is clear that U–Pb dating of relatively large weights (milligrams) consisting of hundreds to thousands of heterogeneous zircon crystals should unavoidably result in their averaged age. At the same time, the possibility of U–Pb dating of single zircon crystals using the precise mass-spectrometry method of isotopic dilution (ID-TIMS) appeared only 10–15 years ago

<sup>a</sup> Zavaritskii Institute of Geology and Geochemistry,  
Ural Division, Russian Academy of Sciences,  
Pochtovyi per. 7, Yekaterinburg, 620219 Russia

<sup>b</sup> Institute of Mineralogy and Economics,  
University of Aachen, Aachen, Germany

<sup>c</sup> Center of Isotopic Studies, Karpinskii All-Russia  
Research Institute of Geology, Srednii pr. 74,  
St. Petersburg, 199106 Russia

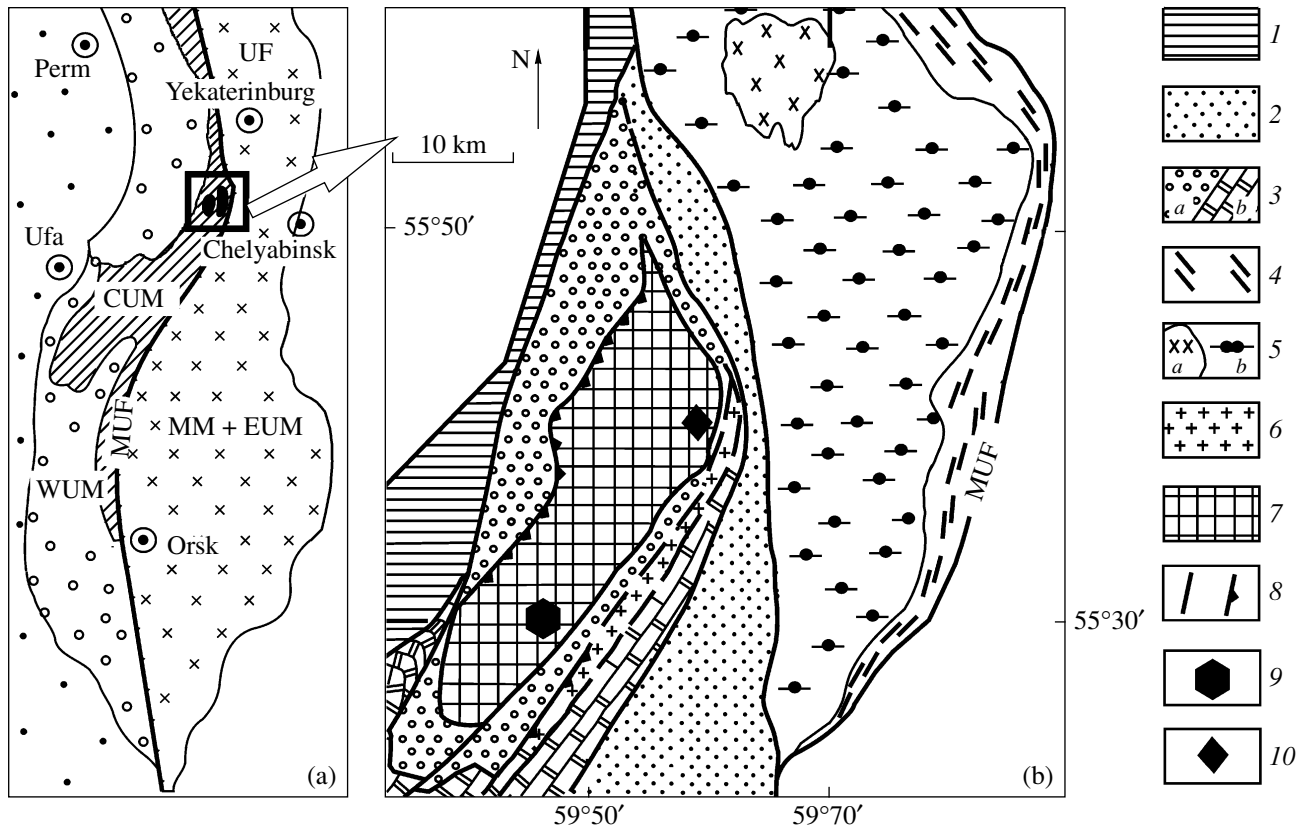


**Fig. 1.** Schematic geological maps demonstrating the position of the Taratash Complex (a) in the structure of the South and Middle Urals and (b) in the northeastern part of the Bashkir Meganticlinorium together with the Aleksandrov and Ufalei complexes (simplified after [8]). (UF) Ural Foredeep; (WUM) West Ural megazone; (CUM) Central Ural megazone; (MUF) Main Ural Fault; (TM) Tagil megazone; (MM) Magnitogorsk megazone; (EUM) East Ural megazone. Rocks: (1) Paleozoic, (2) Middle Riphean, (3) Lower Riphean: (a) Ai Formation, (b) Satka Formation, (4) East Ufalei Complex, (5) West Ufalei Complex: (a) granitoids, (b) amphibolites, (6) Aleksandrov Complex, (7) Taratash Complex, (8) tectonic fractures; (9, 10) sampling sites: Radostnyi Quarry and Mt. Shigir, respectively.

owing to development of highly sensitive mass analyzers and the technique of acid decomposition of analyzed material. The secondary-ion mass-spectrometry (SIMS) methods (SHRIMP, Cameca 1270), which recently have been used widely for in situ study, and the rapidly developing laser ablation method based on mass-spectrometry with inductively coupled plasma (LA ICP-MS) represent more advanced approaches (although less precise than the ID method) to the targeted study of single zircon crystals. Application of these methods provides a unique opportunity for detailed examination of particular areas in zircon crystals with a set of specific features corresponding to the issue under consideration. As follows from the practice of U–Pb dating of single zircon grains, the relevant data are usually less discordant and more accurate<sup>1</sup> as compared with those obtained for large volumes of heterogeneous zircon concentrates.

<sup>1</sup> The accuracy of dates increases, because data points in corresponding plots are localized either near or immediately at the concordia. Therefore, we can minimize errors related to projection of significant discordance at the concordia.

The arguments presented above and previous Nd model ages of approximately 3 Ga obtained for gneisses of the Taratash Complex [9] stimulated this study. We performed the Sm–Nd model (bulk composition) and U–Pb SHRIMP-II (zircon) dating of such rocks. According to [5], they belong to products of granulite metamorphism and represent the oldest rocks in the complex.

The zircons extracted from granite-bearing gneiss (sample T-20, Mt. Shigir) and diorite–gneiss (sample T-22, Radostnyi Quarry) were used for U–Pb dating. The detailed microprobe study using the scanning electron microscope revealed that the examined rocks belong to the granulite facies of metamorphism [8]. Three bulk gneiss samples (samples T-20 and T-22 included) were dated using the Sm–Nd model method.

The zircons were extracted from rocks in line with the traditional procedure. After crushing the initial samples, heavy minerals were extracted by screening through sieves with different-sized mesh, table concentrator, isodynamic magnetic separator, and heavy liquids. Final selection of appropriate zircon grains was

**Table 1.** U–Pb SHRIMP-II zircon data on metamorphic rocks of the Taratash Complex

Crystal, crater	$^{206}\text{Pb}_c$ , %	U, ppm	Th, ppm	$^{232}\text{Th}/^{238}\text{U}$	$^{206}\text{Pb}^*$ , ppm	$^{207}\text{Pb}^*/^{206}\text{Pb}^*$ , ±%	$^{207}\text{Pb}^*/^{235}\text{U}$ , ±%	#	#
22.4.1	0.01	457	46	0.10	175.7	0.1496	0.7	9.23	1.1
22.3.1	0.11	1461	111	0.08	584.5	0.1568	1.1	10.06	1.0
20.3.1	0.91	456	259	0.59	188.0	0.1707	0.6	11.16	1.5
20.2.1	–	280	172	0.63	119.0	0.1826	0.9	12.44	1.4
22.7.1	0.35	412	165	0.41	181.3	0.1975	0.7	13.89	1.2
22.6.1	3.36	270	101	0.39	130.0	0.2214	2.6	16.56	2.9

Crystal, crater	$^{206}\text{Pb}^*/^{238}\text{U}$ , ±%		<i>Rho</i>	$^{206}\text{Pb}/^{238}\text{U}$ , Ma ±%		$^{207}\text{Pb}/^{206}\text{Pb}$ , Ma ±%		<i>D</i> , %
22.4.1	0.4474	0.9	0.82	2384	25.9	2342	12	–1.8
22.3.1	0.4653	0.7	0.70	2463	21.0	2422	19	–1.7
20.3.1	0.4741	1.0	0.67	2502	30.5	2565	10	2.5
20.2.1	0.4942	1.1	0.79	2589	34.9	2676	15	3.4
22.7.1	0.5102	0.9	0.75	2657	29.5	2805	11	5.6
22.6.1	0.5425	1.2	0.41	2794	41.8	2991	42	7.0

Note: Error  $\pm 1\sigma$ . (Pb, Pb\*) total and radiogenic lead, respectively. Errors in calibration relative to standards 0.53%. (#) Correction based on  $^{204}\text{Pb}$ ; (*D*) discordance,  $100 \cdot \{1 - [\text{age}(^{206}\text{Pb}/^{238}\text{U})/\text{age}(^{207}\text{Pb}^*/^{206}\text{Pb}^*)]\}$ ; (*Rho*)  $^{207}\text{Pb}^*/^{235}\text{U}$ – $^{206}\text{Pb}^*/^{238}\text{U}$  correlation coefficient.

carried out by hand under a binocular microscope. The selected specimens were fixed, along with standards 91 500 and TEMORA (with known U–Th–Pb parameters), by Epofix resin at the disc (25 mm across), which was polished until crystals appeared at the surface. Further, using the scanning electron microscope, back-scattered electron images of zircons were obtained, which made it possible, in combination with optical observations in the transmitted and reflected light, to carry out the detailed study of their mineralogical properties.

The crystal sizes range from 60 to 320  $\mu\text{m}$ . Based on the crystal habit, the examined zircons can be divided into several varieties (Fig. 2): isometric (crystals 1, 5, 11), subhedral (20.3, 22.4, 14, 18), and euhedral (20.2, 22.3, 22.7). Their color varies from gray-brown to bright red. Both transparent (2.3, 22.2, 16) and highly opaque (9.17, 18) specimens are also present. Several generations of zircons are distinguished based on their mineralogical features. Zircons of the oldest generation occur as isometric cores (up to 50  $\mu\text{m}$  across) localized largely in central parts of crystals. Optical observations reveal these zircons owing to their dense gray-brown color. Their more reliable identification is provided by scanning electron microscopy (crystal 22.6, BSE image in cathode rays). Moreover, the contours of optical and cathode luminescence boundaries differ from each other. The BSE images of such cores reflect their complex (block-type [10]) structure in contrast to the surrounding two or more shells. For example, crystal 22.6 is characterized by a subhedral internal core and two more perfect envelopes. Differences between images of the central parts and envelopes are also observed in

other crystals. In cathodoluminescence images, their cores have a subeuhedral shape characterized by relatively uniform luminescence, while their optical images demonstrate substantially more intricate superpositions (22.3). Most zircon grains show distinct crushing features (20.3), secondary inclusions (6, 16), and recrystallization (2, 3, 12, 15). Some crystals demonstrate dissolution of internal crystal prisms and irregular zoning due to metamorphic transformations (22.7). Some specimens have curved external contours (9, 10, 12, 18, 22.6), which suggest their specific formation environments. As a whole, the mineralogical properties of the examined zircon assemblage indicate their metamorphic origin and extremely complicated evolution [10].

Careful mineralogical analysis made it possible to select points appropriate for local U–Pb microprobe dating within the examined crystals in order to avoid mixing of isotopic characteristics of polychromous areas in the crystalline lattice of individual zircon grains due to different combinations and concentrations of minor elements, their valence, and structural defects. The parameters of the U–Th–Pb isotopic system of the above-mentioned zircons were measured using the SHRIMP-II high-resolution precision secondary-ion analyzer at the Center of Isotopic Studies, VSEGEI (St. Petersburg), according to the technique described in [11].

Table 1 and Figure 3 present results of in situ U–Pb dating obtained for six zircons. The U and Th contents in the examined varieties range from 270 to 14 611 and from 101 to 270 ppm, respectively. The negative correlation observed between discordance and U con-

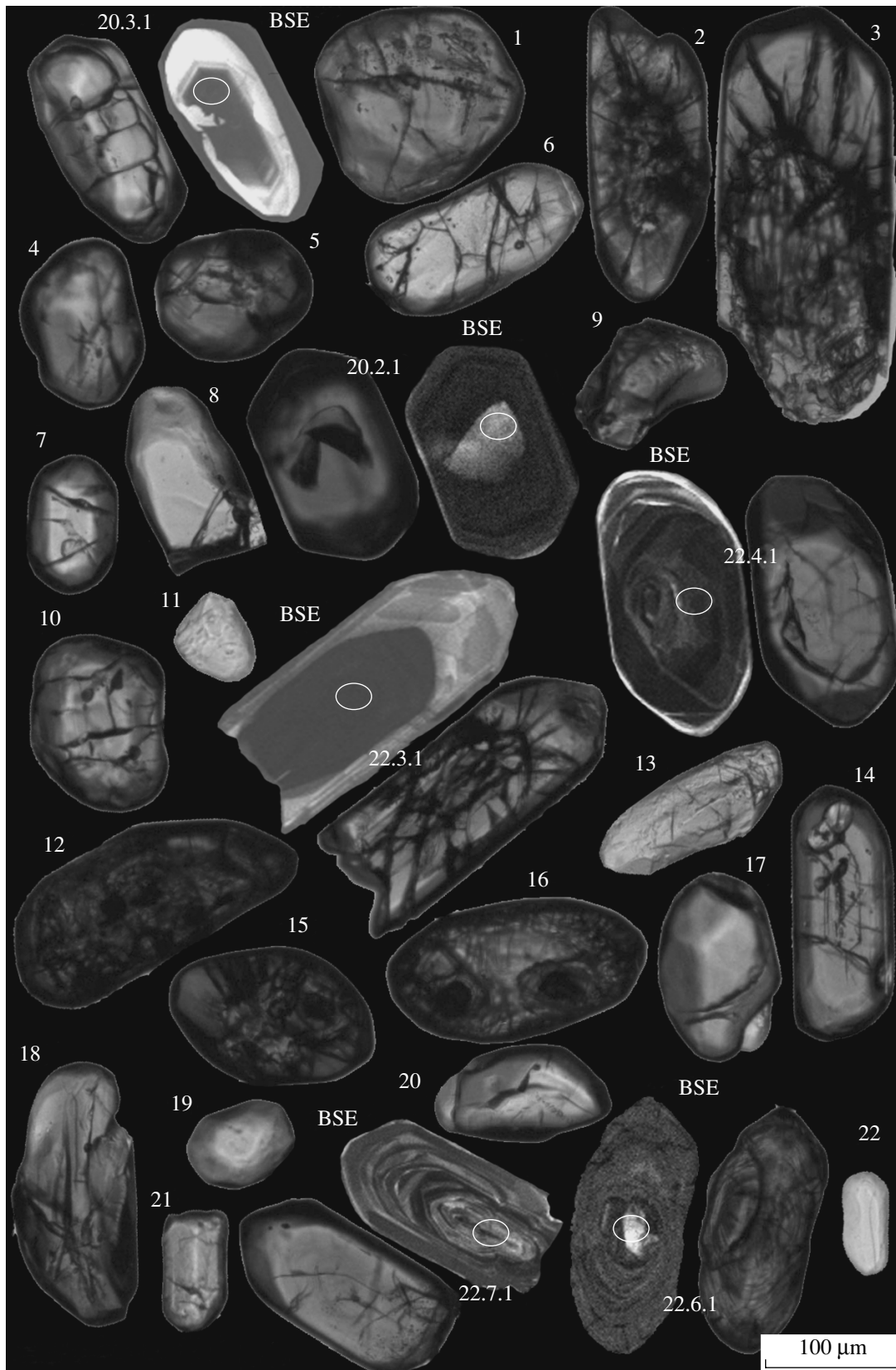


**Fig. 2.** Images in cathode rays (BSE images for crystals 20.3, 20.2, 22.4, 22.3, 22.4, and 22.6) and optical photomicrographs (all others) of zircon crystals from metamorphic rocks of the Taratash Complex. Ellipses demonstrate localization of craters up to 30 μm across and up to 3–4 μm deep formed at the surface of crystals under the impact of the primary oxygen beam of SHRIMP-II.

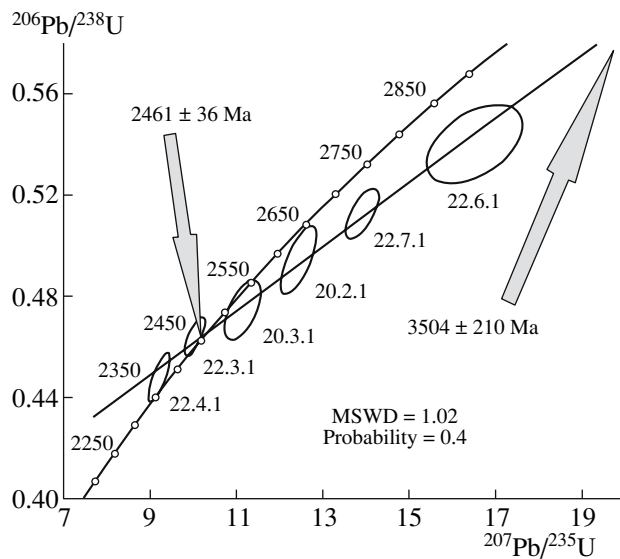


**Fig. 3.** U–Pb data on zircons from metamorphic rocks of the Taratash Complex based on the precision secondary-ion high-resolution microprobe (SHRIMP-II).

tent (Table 1, column D, %) is illustrated by the  $r$  value ( $-0.7$ ), which is somewhat unexpected, since U–Pb data obtained also for zircons from the Taratash Complex [4] demonstrate a reverse correlation.<sup>2</sup> Approximation of U–Pb data presented in Table 1 reveals a distinct isochron fit (MSWD = 1.02) that is characterized by the correspondence probability of 0.4. The positions of data points in the  $^{207}\text{Pb}/^{235}\text{U}$ – $^{206}\text{Pb}/^{238}\text{U}$  plot correspond to the two-stage model of the U–Pb system evolution and yield two age estimates. The lower intercept of discordia with concordia corresponds to the value of  $2461 \pm 36$  Ma, whereas the upper intercept with the regression line corresponds to 3504 Ma. The localization of data points immediately near the lower intercept (points 22.4.1 and 22.3.1 before the intercept; 20.3.1, 20.2.1, 22.7.1, and 22.6.1 after the intercept) determines a significant error value of  $\pm 210$  Ma (Fig. 3).

Table 2 presents the Sm–Nd isotopic system for three samples (T-20, T-22, T-38) from the Taratash Complex. Within the observed error limits, the calculated Nd model ages  $T_{\text{DM}}$  ( $3455 \pm 39$ ,  $3490 \pm 37$ , and  $3645 \pm 34$  Ma, respectively) correspond to the U–Pb zircon date of  $3504 \pm 210$  Ma defined from the upper intercept. The  $\epsilon_{\text{Nd}}$  values calculated for the age of 3.5 Ga demonstrate positive values. The  $\epsilon_{\text{Nd}}$  value of  $+2.6$  determined for sample T-22 practically coincides with that available for the depleted mantle ( $\epsilon_{\text{Nd}} = +2.4$ ), while data points of samples T-20 and T-38 in the  $T$ – $\epsilon_{\text{Nd}}$  plot (Fig. 4) are located slightly above ( $+3.0$ ) and notably below ( $+0.5$ ), respectively. However, this fact gen-

<sup>2</sup> This follows from the analysis of U–Pb data cited in [4, p. 512, Table 1], although the opposite inference is given in the text of the cited work.

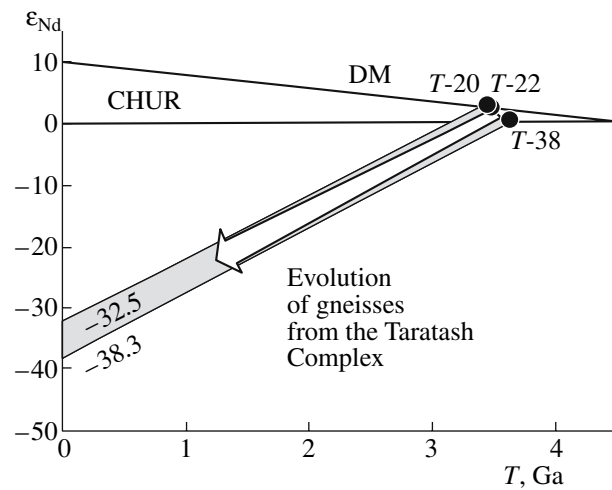


**Fig. 4.** Diagram  $\epsilon_{\text{Nd}}-T$  for three gneiss samples from the Taratash Complex.

erally indicates a substantial role of the mantle component in the protolith.

Thus, the U–Pb SHRIMP-II (zircons) and Sm–Nd (bulk sample) datings of the Taratash polymetamorphic complex have yielded for the first time the oldest (Archean) age of 3.5 Ga in the Urals. Mineralogical features of the examined zircons and available geological observations allow this value to be correlated with granulite metamorphism.

Combined with previous microprobe observations and U–Pb, Sm–Nd, Rb–Sr, and  $^{40}\text{Ar}$ – $^{39}\text{Ar}$  measurements [8, 12, 13], the new U–Pb (SHRIMP-II) and Sm–Nd (ID-TIMS) data allow us to propose the following evolution scenario for the Taratash polymetamorphic complex. The granulite facies of metamorphism corresponding to the temperature interval of  $850$ – $900^\circ\text{C}$  and pressure of 10 kbar was successively replaced by the subsequent regressive stages of amphibolite and greenschist metamorphism. Based on the new U–Pb and Sm–Nd data, the age of granulite metamorphism can be estimated as the Early Archean ( $\sim 3.5$  Ga). Based on the examined zircons, the postgranulite magmatic activity is dated back to  $2461 \pm 36$  (this work),  $2344 \pm 29$ ,  $2044.4 \pm 7.8$  Ma ago [8]. The amphibolite (low-grade) and greenschist facies of regressive metamorphism occurred  $1881 \pm 8$  Ma ago [8]. Manifestations of this metamorphism are recorded in the Aleksandrov and Ufalei complexes [14] located east of the Taratash Complex (Fig. 1). These events were probably related to processes of deformation and granite formation in the East European Craton. The shear zones of the Taratash Complex were probably formed at the same stage. Within the observed error limits, partial homogenization of the Rb–Sr system 1350–1200 Ma ago correlated with anorogenic intraplate magmatism in the Bashkir anticlinorium [15] and preceded the Grenville events, which have not yet been recorded in the Taratash Complex at least in the examined rock variet-

**Table 2.** Sm–Nd data for gneisses of the Taratash Complex

Sample	Sm, ppm	Nd, ppm	$^{147}\text{Sm}/^{144}\text{Nd}$	$\pm 2\sigma$	$f_{\text{Sm}/\text{Nd}}$	$^{143}\text{Nd}/^{144}\text{Nd}$	$\pm 2\sigma$	$\epsilon_{\text{Nd}}(0)$	$^*\epsilon_{\text{Nd}}(3.5)$	$T_{\text{DM}}$ , Ma	$\pm\Delta T_{\text{DM}}$ , Ma
T-22	2.19	12.0	0.1101	0.0009	–0.44	0.510761	0.000016	–36.6	+2.6	3490	37
T-38	1.43	7.82	0.1109	0.0008	–0.44	0.510673	0.000013	–38.3	+0.5	3645	34
T-20	1.96	10.0	0.1182	0.0009	–0.40	0.510971	0.000015	–32.5	+3.0	3455	39

Note:  $^*\epsilon_{\text{Nd}}(3.5)$  recalculated for the age of 3.5 Ga.  $^{147}\text{Sm}/^{144}\text{Nd}$  for the uniform chondrite (CHUR) and depleted reservoirs (DM) is 0.1967 and 0.2140, respectively;  $^{143}\text{Nd}/^{144}\text{Nd}$  is 0.512636 and 0.513160, respectively. The contents and isotopic compositions of Sm and Nd were determined at the Institute of Geology and Geochemistry, Ural Division, Russian Academy of Sciences, by the method of isotopic dilution and using mixed ( $^{149}\text{Sm} + ^{150}\text{Nd}$ ) spike and further mass-spectrometric analysis with a Finnigan MAT-262 multi-collector solid-phase analyzer in the static regime. Reproducibility of measured ratios  $^{147}\text{Sm}/^{144}\text{Nd}$  and  $^{143}\text{Nd}/^{144}\text{Nd}$  was controlled using standards BCR-2 and La Jolla, respectively.

ies. Based on the  $^{40}\text{Ar}$ – $^{39}\text{Ar}$  and Rb–Sr estimates, the Taratash and Aleksandrov complexes were exhumed approximately 300 Ma ago [8]

#### REFERENCES

1. E. V. Bibikova, *U–Pb Geochronology of Early Stages in the Development of Ancient Shields* (Nauka, Moscow, 1989) [in Russian].
2. T. M. Kusky and A. Polat, *Tectonophysics* **305**, 43 (1999).
3. V. N. Puchkov, *Paleogeodynamics of the South and Middle Urals* (Dauriya, Ufa, 2000) [in Russian].
4. A. A. Krasnobaev and N. V. Cherednichenko, *Dokl. Earth Sci.* **400**, 145 (2005) [*Dokl. Akad. Nauk* **400**, 510 (2005)].
5. *Petrology and Iron Ore Deposits of the Taratash Complex* (UNTs AN SSSR, Sverdlovsk, 1978) [in Russian].
6. A. I. Tugarinov, E. V. Bibikova, A. A. Krasnobaev, and V. A. Makarov, *Geokhimiya*, No. 4, 501 (1970).
7. M. A. Garris, *Stages of Magmatism and Metamorphism in the Pre-Jurassic History of the Urals and Adjacent Areas* (Nauka, Moscow, 1977) [in Russian].
8. S. Sindern, R. Hetzel, V. A. Schulte, et al., *Int. J. Earth Sci.* **94**, 319 (2005).
9. Y. L. Ronkin, M. Portugal Ferreira, and O. P. Lepikhina, in *Abstract Volume of South American Symposium on Isotope Geology* (Sao Paolo, 1997), pp. 189–203.
10. F. Corfu, J. M. Hanchar, P. W. O. Hoskin, and P. Kinny, in *Zircon. 2003* (Miner. Soc. Am., Washington D.C., 2003), pp. 469–500.
11. Yu. L. Ronkin, D. I. Matukov, S. L. Presnyakov, et al., *Litosfera*, No. 1, 135 (2005).
12. Yu. L. Ronkin, S. Sindern, U. Kramm, et al., in *Isotope Geochronology in Solving Problems of Geodynamics and Ore Genesis. Materials of the 2nd Russian Conference on Isotope Geochronology* (IGGD RAN, St. Petersburg, 2003), pp. 420–424 [in Russian].
13. Yu. L. Ronkin, S. Sindern, U. Kramm, et al., in *Structure, Geodynamics, and Mineragenic Processes in the Lithosphere. Materials of Internal Scientific Conference* (Geoprint, Syktyvkar, 2005) pp. 311–312 [in Russian].
14. R. Hetzel and R. Romer, *Geol. Mag.* **136**, 593 (1999).
15. Yu. L. Ronkin, O. P. Lepikhina, and O. Yu. Popova, in *Yearbook-2004* (IGG UrO RAN, Yekaterinburg, 2005), pp. 211–220 [in Russian].